Advances in Science and Technology Research Journal

Advances in Science and Technology Research Journal, 2026, 20(3), 373–386
https://doi.org/10.12913/22998624/214593
ISSN 2299-8624, License CC-BY 4.0

Received: 2025.09.26
Accepted: 2025.11.29
Published: 2026.02.01

Experimental investigations on analysis of variance analysis of hardness and thermal conductivity of AL7475 reinforced silicon nitride and graphite

Sharan Tej Reddy[1*], Murali Mohan Ramakrishnappa[2], Vijay Kumar Shankar[3], Vijee Kumar Dr[4]

[1] Research Scholar, Department of Mechanical Engineering, Government Engineering College, Hassan, 573201, Karnataka, India
[2] Department of Mechanical Engineering, Government Engineering college, Hassan, 573201, Karnataka, India
[3] Department of Robotics and Artificial Intelligence, Nitte Meenakshi Institute of Technology, Nitte (Deemed to be University) Bangalore, Karnataka, India
[4] Department of Mechanical Engineering, REVA University, Bangalore, Karnataka, India
* Corresponding author's e-mail: sharanreddy024@gmail.com

ABSTRACT

This study investigates the mechanical and tribological behavior of Al7475-based metal matrix composites (MMCs) reinforced with varying proportions of silicon nitride (Si_3N_4) and graphite (Gr), developed through stir casting. The present study highlights the beneficial impact of graphite and Si_3N_4 reinforcement on the Al7475 wear performance to determine the hardness and thermal conductivity of the composites. This study examines Al7475-based MMCs reinforced with 3–12% Si_3N_4 and graphite via stir casting. The optimal 5% Si_3N_4–5% Gr hybrid composite achieved superior Hardness (74.1) and the Thermal conductivity for 5% Si_3N_4–5% Gr is 242.7 W/(m°C). Microstructural analysis revealed that the inclusion of Si_3N_4 improved grain refinement and hardness, while graphite contributed to enhanced lubrication and wear resistance. SEM/EDS confirmed uniform dispersion, while fractography revealed a ductile-to-brittle transition with higher reinforcement. ANOVA (R^2 > 89% for Thermal conductivity, > 98%) validated reinforcement significance, highlighting that optimal ratios enhance performance, whereas excess causes agglomeration and reduced ductility. The findings confirm that an optimal hybrid reinforcement ratio effectively enhances mechanical strength and thermal conductivity, while excessive reinforcement leads to agglomeration, reduced ductility, and inferior performance.

Keywords: Al7475, Si_3N_4, ANOVA, graphite, hardness, thermal conductivity.

INTRODUCTION

In recent times, lightweight MMC'S have improved and are now applicable in several automotive and aerospace industries. Metal matrix composites (MMCs) comprising metallic matrix and a distributed reinforcing phase, which is either ceramic or metallic. Hybrid metal matrix composites (HMMCs) comprise a metallic matrix and various evenly distributed metallic or ceramic constituents. The matrix serves as a conduit for load transfer and distribution. Different matrix types, reinforcements, and manufacturing techniques can affect load transfer. The mechanical and thermal ageing properties of a composite material are greatly influenced by the selection of reinforcing material. In addition to its enhanced specific strength and corrosion resistance, hard second phase particles may be included into alloy matrices to form MMCs. Ibrahim et al. (1991) [1].

Suvarna Raju et al. showed that Al_2O_3 reinforcement significantly enhanced Cu-based composites via FSP, with volume fraction as the key factor, improving strength, hardness, toughness, and ductile fracture behavior through grain refinement and dislocation pinning [2]. Moustafa

et al. fabricated AA7075/hBN–carbide hybrid composites via FSP, achieving strong matrix bonding, grain refinement, and remarkable property gains—40% higher hardness, 26.5% higher compressive strength, and 24× wear resistance—attributed to hBN's self-lubrication and grain boundary pinning [3]. FSP-produced AA6061/Al_2O_3–BN hybrid and mono nanocomposites showed ~29× grain refinement and ~100% gains in strength and hardness over base alloy, attributed to uniform nanoparticle dispersion and synergistic effects. While ceramic reinforcements reduced conductivity, strain rate, and thermal expansion, the hybrid composite exhibited the lowest values, suiting structural applications requiring high strength and thermal stability [4]. Gugulothu et al. (2021) studied ECM of stir-cast Al5086/SiC/fly ash composites using Taguchi's L16 design, finding feed rate (47%) most influential on MRR, followed by electrolyte concentration (23.5%) and voltage (17.6%). Higher feed rate and voltage improved MRR, while excess electrolyte reduced it, confirming ECM's suitability for hybrid Al composites [5]. Mazo et al. fabricated dense SiOC–Si_3N_4 composites via SPS with carbon nanofibers, forming SiC nanostructures and graphene-like carbon in-situ. The hybrid microstructure offered high oxidation resistance (≤1400 °C), low thermal expansion (1.26×10^{-6} K^{-1}), improved conductivity (33.6 S/m electrical, 1.91 W/m·K thermal), and high solar absorptance (95.8%), making them promising for heat absorber and high-temperature applications [6]. Sharath et al. reviewed ceramic-reinforced Al hybrid composites, highlighting enhanced strength, wear resistance, and thermal stability from reinforcements like graphite and B_4C, making them suitable for automotive, aerospace, and manufacturing applications. The study also noted challenges with interfacial bonding, ceramic dispersion, ductility, and processing, suggesting further research to boost performance in critical components [7]. Suvorova et al. studied LPBF-fabricated AlSi10Mg composites with AlN and ZrN, showing poor wetting of AlN caused porosity and strength loss, while ZrN enabled reactive wetting, forming $Zr(Al,Si)_3$ intermetallic that enhanced tensile strength and hardness (up to 135 HV0.1) at 0.5–1 vol%. Excess ZrN, however, promoted brittle phases and reduced strength, underscoring the critical role of wetting in tailoring AMCs [8]. Khalid et al. reviewed Al7075 and its composites for aerospace, noting that stir casting with ceramic/nanoparticle reinforcements enhances mechanical, tribological, and microstructural properties. Despite challenges like agglomeration and poor dispersion, stir casting remains cost-effective. The study also highlighted the growing role of machine learning in predicting properties and optimizing processing for next-generation lightweight AMMCs [9]. Reddy et al. studied stir-cast Al-7475 with 10 wt% fly ash and 3–12 wt% graphite, finding strength and hardness improved up to 9 wt% (64.6 HRB, 255.6 MPa) before declining. Graphite reduced CTE and thermal conductivity, though both increased with temperature (50–300 °C), reaching 135 W/m·K at 12 wt%. Optimal graphite reinforcement enhanced the composites' strength and thermal stability [10]. Stir-cast Al7075/n-TiB_2 nanocomposites (1–2.5 wt%) showed improved density, hardness, tensile strength, and wear resistance, with peak gains at 2.5 wt% (hardness ↑14%, strength ↑9%, wear resistance ↑20%). Fractography revealed ductile failure, while pin-on-disc tests confirmed reduced oxidative wear, making the composites suitable for structural applications [11]. Das et al. fabricated Al6082/4 wt% B_4C composites via stir casting, achieving a pore-free, uniformly reinforced matrix. Compared to base alloy, hardness, tensile strength, yield strength, and toughness improved significantly. Fractography revealed strain-localized voids, confirming enhanced strength and toughness, making the composite promising for automotive applications [12]. Kumar Gopalan et al. produced Al2214/8 wt% n-B_4C composites (~500 nm) via stir casting with preheated reinforcement, achieving uniform dispersion verified by SEM, EDS, and XRD. Compared to base alloy, hardness, yield strength, UTS, and compressive strength improved significantly, while ductility decreased [13]. Veeresha et al. developed Al2618/B_4C (2–8 wt%, 63 μm) composites via stir casting, showing uniform reinforcement distribution and notable gains in hardness, tensile, yield, and compressive strengths with slight ductility loss. Wear resistance improved with B_4C content despite higher wear at greater loads and speeds, making the composites suitable for aerospace applications [14]. A DOE optimizes information acquisition while minimizing resource expenditure, therefore enhancing the information obtained [15]. Montgomery [16] regards the DOE as a potent instrument due to its capacity to concurrently and efficiently examine the impacts

of various factors within a system or process, hence enhancing comprehension. The process transforms certain inputs into outputs, yielding one or more answers using a mix of equipment, procedures, personnel, and additional resources.

Although extensive work has been done on aluminum matrix composites, research on Al7475 reinforced with silicon nitride (Si_3N_4) and graphite (Gr) remains limited. This hybrid reinforcement offers potential to enhance the alloy's mechanical and thermal properties. The present study addresses this gap by investigating the effect of varying Si_3N_4 and Gr weight percentages in the Al7475 matrix, focusing on hardness and thermal conductivity. Data from previous studies are used for comparison, and statistical models are developed to establish mathematical correlations between reinforcement composition and material performance. These models provide insights for optimizing composite design in future aerospace and engineering applications.

MATERIALS AND METHODS

The selection, characterization, and assessment of aluminium alloy reinforced [21–24] with Graphite and Si_3N_4 reinforcements for various combinations ranging from 3%, 5%, 6%, 10% to 12% for both the combinations were considered in the current experimental work. The purpose of this procedure is to examine how the Hardness and predictability thermal Conductivity of these materials are impacted by the addition of Graphite and Si_3N_4 (Figure 2). Al7475 with Graphite and Si_3N_4 reinforcements was chosen as the base material in different distinct aluminium (Al7475) concentrations with a detailed methodology is shown in Figure 1. SEM and EDS analyses [25–28] are used to examine the structural and elemental changes in the machined Specimens. Mechanical properties such as hardness and thermal conductivity are determined. The detail chemical composition of the Pure AL7475 I given in Table 1.

Figure 1 presents a systematic approach in the present study to assess mechanical and thermal properties of Al7475–Si_3N_4/Gr metal matrix composites. The process began with selecting appropriate materials: Al7475 alloy was chosen as the base metal due to its high strength, lightweight, and good corrosion resistance, and Si_3N and graphite (Gr) were added to strengthen, improve the wear resistance, and enhance the heat transfer properties of the material. Each reinforcement was accurately weighed for different weight percentages. Composites were prepared using the stir casting method, which helps the reinforcement particles to be properly distributed in molten aluminum. Parameters such as stirring speed, temperature, and feed rate were controlled to ensure uniform mixing. The samples were then allowed to solidify, followed by machining and polishing according to ASTM standards for

Table 1. Chemical compositions of Al-7475 alloy

Content	Cu	Mg	Si	Mn	Sn	Ti	Zn	Cr	Al
Wt. %	1.29	2.15	0.08	0.03	0.01	0.05	5.92	0.21	Rem

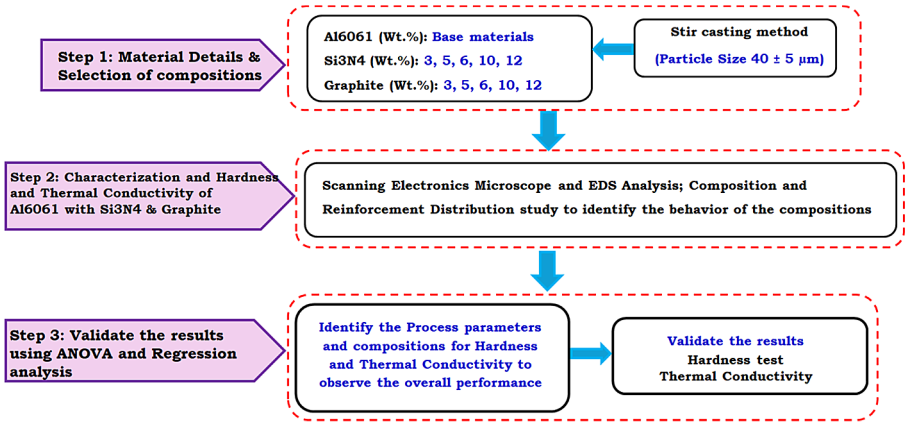

Figure 1. Methodology of the present investigations

Figure 2. Specimen preparation as per the standard for Al7475 with graphite and Si_3N_4

hardness and thermal conductivity testing. Hardness tests (Vickers or Brinell) were conducted to measure the resistance of the material to indentation, and multiple readings were averaged for accuracy. Thermal conductivity was tested using the Disc method to determine how well the material conducts heat. Finally, the experimental results were compared with studies in the literature in order to validate the findings and observe how changes within Si_3N_4 and Gr content affected hardness and thermal conductivity. The final steps in the analysis included the development of statistical and regression models in order to build a mathematical relationship between the composition and the properties of composites, helping predict and optimize their performance.

Figure 3. Specimen preparation as per the standard

Experimental investigations

Investigations were conducted using an L9 (Table 2) orthogonal array [17–20] design with Si_3N_4 and graphite reinforcements (Figure 3 and 4). The composites were fabricated via stir casting (Figure 5 and 6), and Specimens with varying reinforcement levels were prepared (Figure 6). Five distinct compositions 3%, 5%, 6%, 10%, and 12% were tested to evaluate the Hardness and thermal conductivity of Al7475/Si_3N_4/Gr hybrid composites

Table 2. Taguchi L_9 Orthogonal design for different combinations of Al7475 reinforced with Si_3N_4 and Graphite

Sl/No	AL7475	Si_3N_4	Graphite	Type of composites	Hardness test
0	100	0	0	As-cast Alloy	62.1
1	94	6	0	Si_3N_4 only	65.4
2	94	0	6	Graphite only	67.7
3	94	3	3	Hybrid	68.4
4	90	0	10	Graphite only	68.1
5	90	10	0	Si_3N_4 only	72.1
6	90	5	5	Hybrid	74.1
7	88	12	0	Si_3N_4 only	72.4
8	88	0	12	Graphite only	69.5
9	88	6	6	Hybrid	70.2

Figure 4. Specimen preparation as per the standard

Figure 5. Specimen preparation as per the standard

(Figure 7 and 8). Detail schematic representation of the detail investigations in the form of block diagram is shown Figure 9. Si_3N_4/Gr are chosen as reinforcements to improve these metals' qualities. Al7475 formulations with varying percentages of Si_3N_4/ Gr are characterized. Energy-dispersive X-ray spectroscopy (EDS) and scanning electron

Figure 6. Specimen preparation as per the standard

microscopy (SEM) are two characterization techniques that can be used to examine the chemical composition and microstructure. The mechanical characteristics of the produced alloys with different percentages are tested, including their hardness and thermal conductivity.

RESULTS

In this study, Al7475 was reinforced with 3–12% Si_3N_4 and graphite (hybrid) using the Taguchi L9 designed fabricated by stir casting. SEM and EDS analyses confirmed uniform reinforcement distribution, were evaluated for all combinations. Optical microscopy and SEM/EDS analyses revealed that Si_3N_4 reinforcement refined grains and improved bonding up to 10% (Figure 11), but excessive addition (12%) caused clustering, voids, and reduced ductility. Graphite enhanced lubrication and wear resistance, though higher contents led to agglomeration and porosity. Hybrid reinforcement (5% Si_3N_4 + 5% Gr) achieved uniform dispersion, balanced strength, and wear resistance,

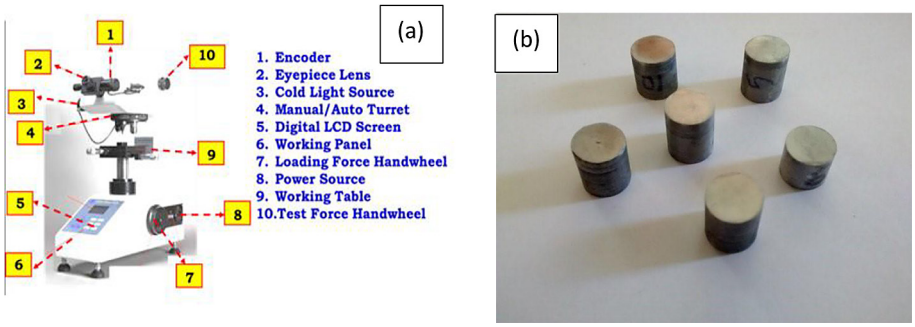

Figure 7. (a) Vickers hardness tester setup. (b) specimen size and shape

Figure 8. Schematic of thermal conductivity setup

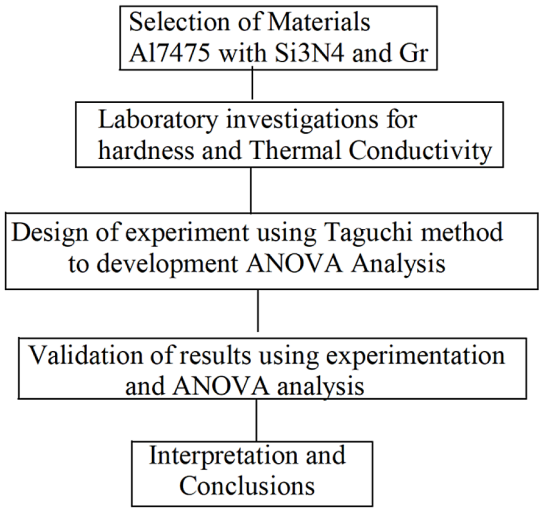

Figure 9. Schematic block diagram of present investigations

while excessive hybrid loading (6% + 6%) showed severe clustering and poor toughness (Figure 10).

Optical microscopy was used to study the microstructure of 7475 aluminum alloy composite fabricated ones. The Specimens were polished with emery papers (400–1500 grit) and alumina paste, followed by etching using Keller's reagent to expose grain boundaries and reinforcement distribution. Grain structure, dispersion of reinforcement (Si_3N_4, graphite), porosity, and microstructural uniformity are studied through the analysis. In contrast to the coarse, equiaxed grains of the unreinforced alloy, the reinforced Specimens had finer grains and better dispersion, which directly affect mechanical and tribological properties. Reinforcement with Si_3N_4 causes the microstructure to change considerably. At 6%, fine particles are well dispersed, encouraging grain refinement, good interfacial bonding, and low porosity. At 10%, additional grain refinement is noted, although minor agglomeration is seen close to grain boundaries. At 12%, there is pronounced clustering, irregular grain boundaries, and micro voids. Although higher Si_3N_4 content increases strength at first, over addition decreases ductility and induces stress concentrations, citing the necessity for optimum reinforcement levels. Graphite displays a flaky, layered structure with high surface area, ideal for lubrication if well dispersed. EDS analysis confirms elemental purity, with distinct Si and N peaks for Si_3N_4 and a dominant C peak for graphite, validating the quality of the reinforcement powders used in the composites (Figure 12 (a–b)). All the compositions of SEM is represented in Figure 10 (a–j). The fractography of failed composite specimens revealed features typical of ductile failure, such as equiaxed dimples By microscopy examination of the fracture surfaces during fractographic analysis, the mode of failure could be identified: numerous microvoids and dimpled rupture areas indicate that large plastic deformation preceded the fracture of the material rather than brittle cleavage. Such a ductile morphology may suggest that Si_3N_4 and graphite reinforcement particles improved matrix integrity and delayed crack initiation and propagation, consistent with earlier studies in ductile metal alloy fractography.

Hardness

Alloy hardness was assessed by using a Vickers micro hardness tester. The hardness tests were carried out by applying a force of 1 Kg-f. Table 2 represents hardness test results of Al7475/Si_3N_4/Gr MMCs with different percentages (Around 10 Specimens) of Si_3N_4/Gr respectively. The higher values of Si_3N_4/Gr and even for the hybrid combinations have high hardness value. In the investigation of surface hardness, the Vickers microhardness test was applied with an operating load of 1 kgf. This test was performed under conditions that were in compliance with the code for obtaining accurate and repeatable surface hardness by microindentation test methods for aluminum-based metal matrix composites. Even though this loading condition does not accurately simulate actual service loads that are usually imposed on

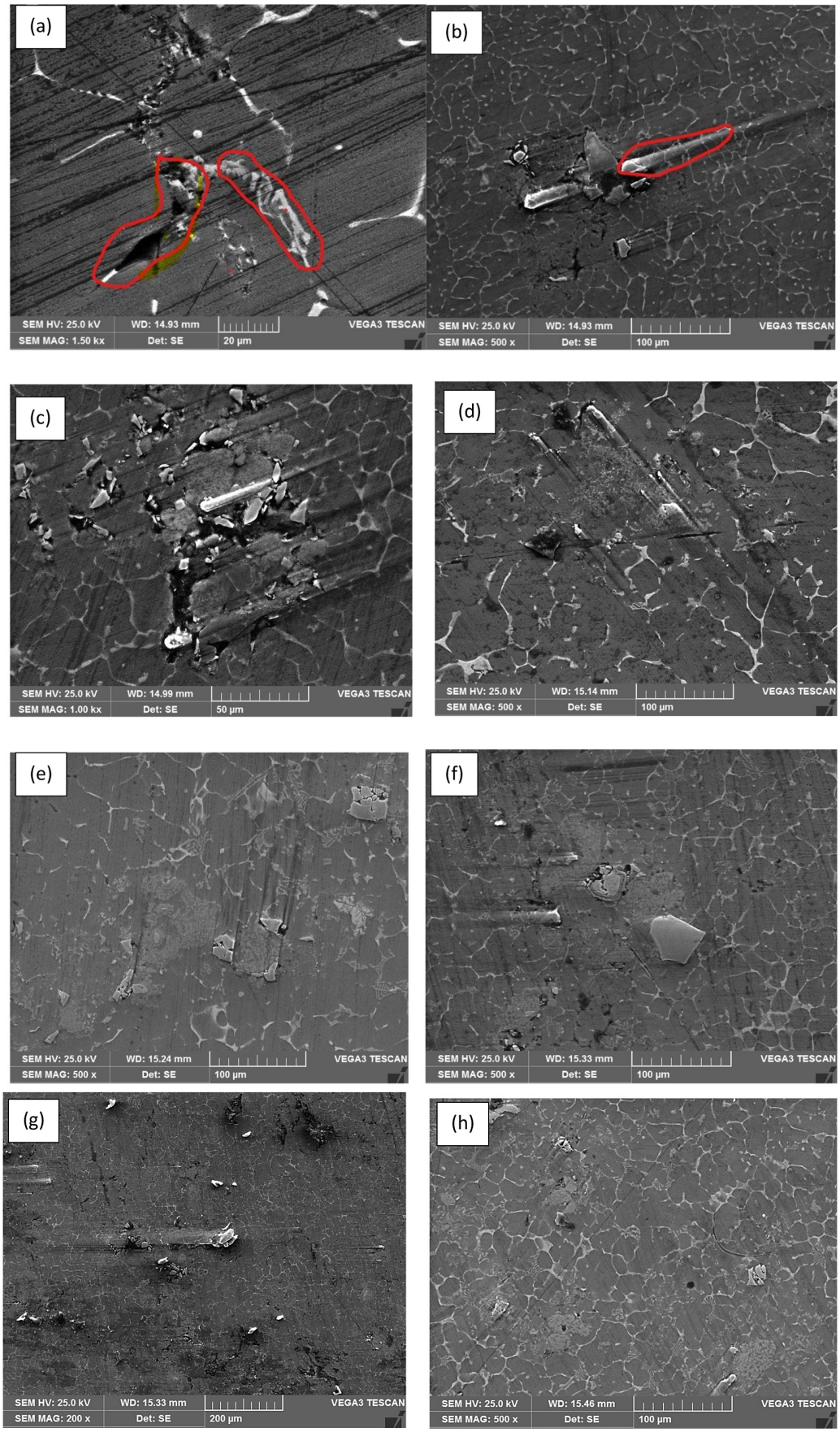

Figure 10. SEM analysis for all the combination of Si_3N_4 and Graphite (a) 0% (b) 6% Si_3N_4 (c) 10% Si_3N_4 (d) 12% Si_3N_4 (e) 6% Graphite (f) 10% Graphite (g) 12% Graphite (h) 3% Si_3N_4+ 3% Graphite (i) 5% Si_3N_4+ 5% Graphite (j) 6% Si_3N_4+ 6% Graphite

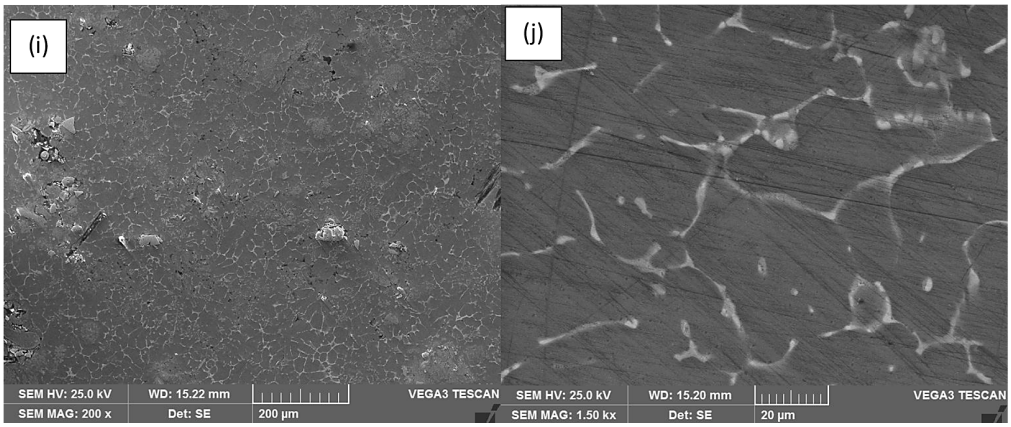

Figure 10. Cont. SEM analysis for all the combination of Si_3N_4 and Graphite (a) 0% (b) 6% Si_3N_4 (c) 10% Si_3N_4 (d) 12% Si_3N_4 (e) 6% Graphite (f) 10% Graphite (g) 12% Graphite (h) 3% Si_3N_4+ 3% Graphite (i) 5% Si_3N_4+ 5% Graphite (j) 6% Si_3N_4+ 6% Graphite

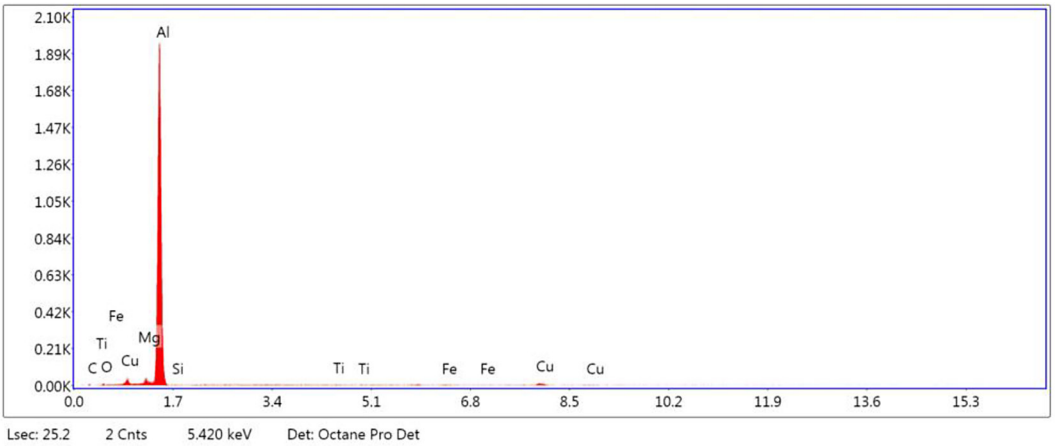

Figure 11. Specimen EDS analysis for all the combination of Si_3N_4 and Graphite

aerospace components, it is a consistent and controlled way to evaluate the material for resistance to local plastic deformation. This load level was optimized to avoid excessive indentation depth or matrix cracking, which can occur at higher loads in particle-reinforced composites. Although the test essentially simulates a compressive load condition imposed in a very small region rather than full-scale operational stresses, the applied load characterizes the surface strength and resistance against wear, important properties in view of contact and bearing stresses in aerospace and structural applications. The operating load thus fairly represents the composite's micro-mechanical response and its resultant resistance to surface deformation and wear during service conditions. Table 2 presents the hardness of Al7475 alloy and its Si_3N_4/Gr composites under varying die pre-heat temperatures (125–280 °C) and stirring speeds (400–450 rpm). The lowest hardness was observed for 2% Si_3N_4, the highest for 5% Si_3N_4/Gr, and an intermediate value for 12% Si_3N_4. On average, hardness increased by 11.32% (12% Si_3N_4) and 14.57% (5% Si_3N_4/Gr), compared to the base alloy. While hardness generally rose with reinforcement, values peaked at 5% Si_3N_4/Gr (Figure 13) and declined slightly at 12% for Gr (Table 2) due to particle agglomeration weakening the matrix–reinforcement bond, consistent with prior studies.

Thermal conductivity of Al7475 alloy reinforced with graphite and Si_3N_4 composites

In this study, thermal conductivity was measured using a hot plate system in accordance with ASTM C177-97 (Standard Test Method for Steady-State Heat Flux Measurements and Thermal Transmission Properties using the Guarded

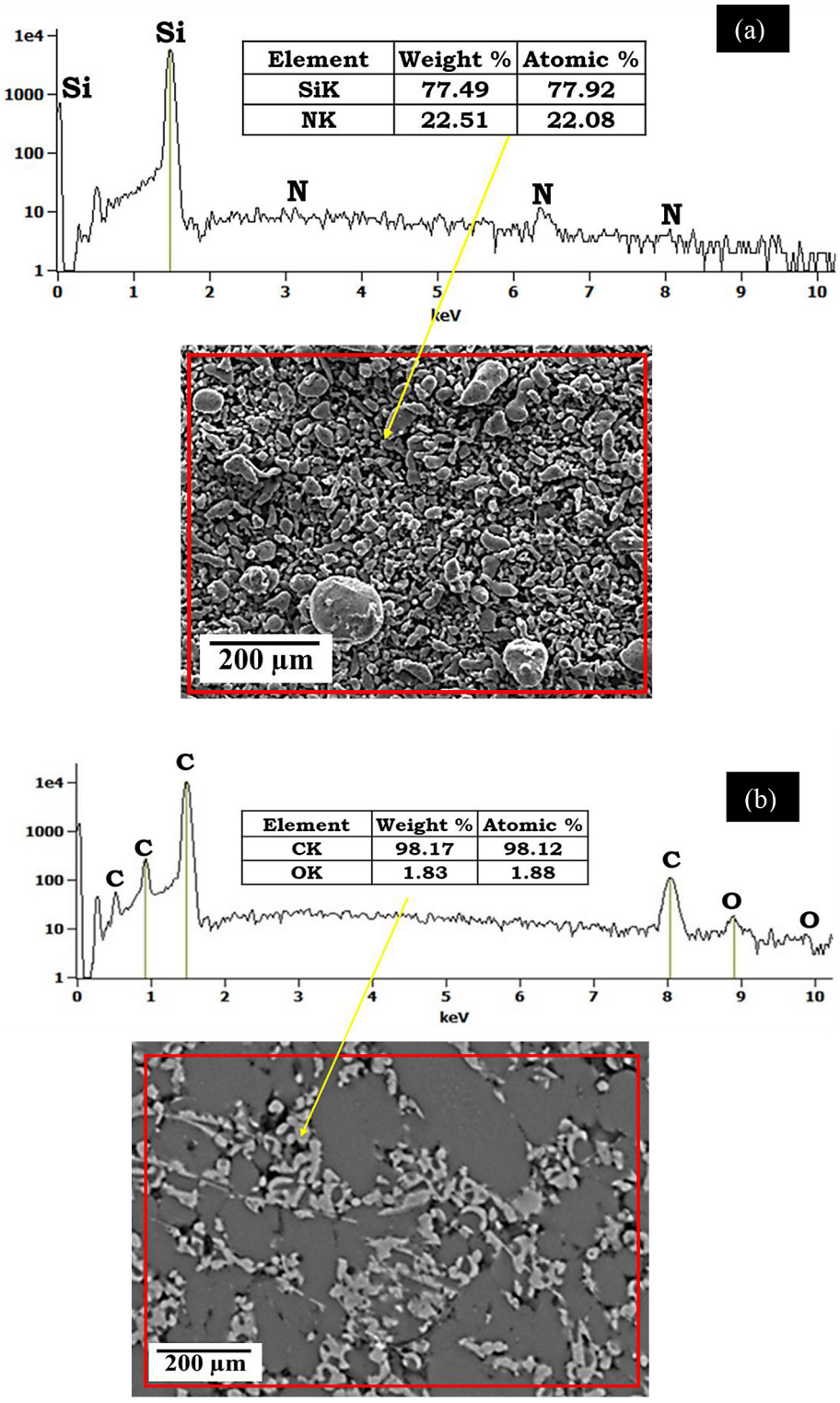

Figure 12. EDS Analaysis of (a) Si_3N_4 and (b) Graphite for the present investigations

Hot Plate Apparatus). The Specimens (around 10 numbers) prepared for all combinations, with uniformly drilled 4 mm thermocouple holes, are shown in Figures 14 and 15. The complete set of Specimen combinations is summarized in Table 3.

Table 3 presents the performance of specimens 6A1–6C3 under varying electrical inputs, showing voltage, current, power, specimen and water temperatures, mass flow rate, thermal conductivity, and heat flux. Results indicate that optimal thermal conductivity occurs at the lowest power input (50 V, 0.2–0.22 A). This demonstrates that lower electrical inputs enhance thermal conductivity, making the materials more suitable for

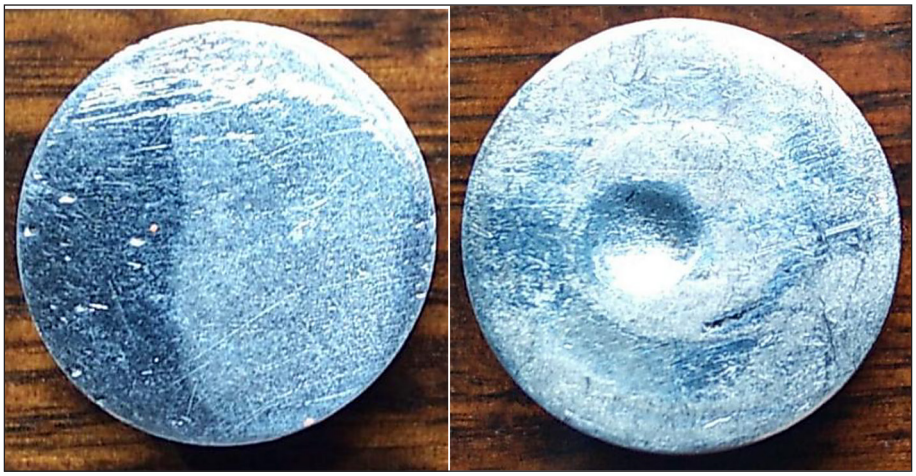

Figure 13. Specimen Vickers hardness of before and after the test for the combination of Si_3N_4 and Graphite with AL7475

Figure 14. Prepared specimens for the thermal conductivity test with a standard size

Table 3. Specimen compositions

Specimen	Al6005	Si_3N_4	Graphite
Pure	100	0	0
6A1	99.5	6	0
6A1	99	0	6
6A1	98.5	3	3
6B1	99.5	0	10
6B1	99	10	0
6B1	98.5	5	5
6C1	99.5	12	0
6C1	99	0	12
6C1	98.5	6	6

thermal management (Table 4). Al6005 provides a balance of strength and conductivity, while uniformly dispersed Si_3N_4/Gr particles further improve heat transfer by reducing thermal resistance and ensuring efficient pathways (Figure 16).

Specimen determination of thermal conductivity (K):

$$Q = -K \times A \times \frac{dT}{dX} \quad (1)$$

where: Q is heat flux K – (1) 50˚, (2) 70˚, (3) 90˚, A is area $A = \pi dl$, $\frac{dT}{dX}$ = slope of the graph.

Determination of thermal conductivity (K) for 6A1 (Specimen calculation)

- At 50°

$$K = -\frac{Q}{A \times (\frac{dT}{dX})}$$

$$Q = M_X \times C_{PW} \times (T_{OUT} - T_{IN})$$

$$Q = 0.012 \times 4178 \times (40.1 - 35.6)$$

$$Q = 225.612 \text{ W/m}^2$$

$$A = \pi \times d \times l$$

Figure 15. Prepared Specimens with Thermocouple holes to perform temperature measurement throughout the specimens

Table 4. Thermal conductivity results for all combinations considered

Specimen	Volts V	Current I	Power Watts	Specimen temperature °C						Water temperature °C		Mass flowrat Lpm	Thermal conductivity W/(m-C)	Heat flux W/ m^2
				T1	T2	T3	T4	T5	T6	T7	T8			
6A1	50	0.22	11	39.3	37.6	36.2	35.2	34.2	33.4	30.6	40.1	0.1	274.63	225.612
6A1	70	0.33	23.1	49	45.2	42.3	40.1	37.8	35.9	31.9	41.5	0.1	271.08	481.31
6A1	90	0.33	23.1	67.7	59.8	53.8	49.3	44.6	40.5	32.7	42.1	0.1	127.94	471.28
6B1	50	0.22	11	34.4	33.7	32.9	32.3	31.8	31.3	30.7	35.1	0.1	268.53	220.59
6B1	70	0.3	21	43.6	41.3	38.8	37.1	35.3	33.8	31.5	36.9	0.1	212.84	270.73
6B1	90	0.4	36	54.4	50.2	45.9	43	39.7	36.8	32.3	38.5	0.1	137.99	310.84
6C1	50	0.22	11	37.8	36.5	35.3	34.4	33.4	32.7	32.9	36.1	0.1	242.17	160.44
6C1	70	0.3	21	46.3	43.5	40.9	38.9	36.8	35.1	32	37.2	0.1	182.18	260.71
6C1	90	0.4	36	61.9	56.3	51.1	47.1	42.7	39.2	30.5	38.1	0.1	133.14	381.03

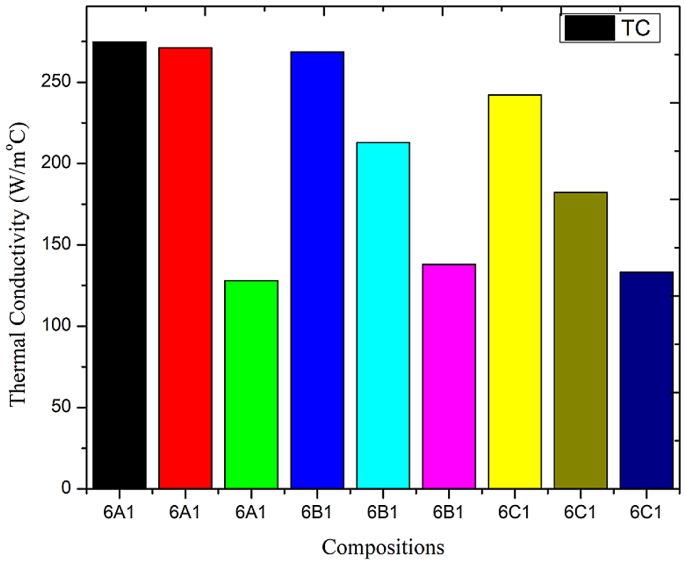

Figure 16. Thermal conductivity of Al7475 reinforced with Si_3N_4/Gr for different combinations considered

$$A = \pi \times 0.025 \times 0.27$$

$$A = 0.0212 \text{ m}^2$$

$$\frac{dT}{dX} = 38.75$$

$$K = \frac{225.612}{0.0212 \times 38.75}$$

$$K = 274.63 \text{ W/m-C}$$

ANOVA analysis

ANOVA analysis was performed on the experimental data to evaluate the influence of variables such as Al7475, Si_3N_4 and Graphite on hardness and thermal conductivity for different load condition. The Taguchi L9 orthogonal array was employed to assess the combined effect of these parameters on Mechanical and thermal property, and ANOVA was used to determine the percentage contribution of each factor. The correlation coefficients for all nine trials were calculated, establishing the relationship between the variables. The detailed results are presented below, and ANOVA table represented the percentage contribution with a P value to identify the significant parameters are provided in Tables 5–6.

For all combinations, experimental and anticipated values are graphed for all properties considered as depicted in Figure 17. The error is evident is less than 5% (Table 5 and 6) and anticipated points match measured levels closely. Hence the predicted equation is good predictive capability with acceptable accuracy. Finally the addition of grain refiners/modifier improves the hardness and thermal conductivity for each combination explored. Figures 14 in this study provide a set of

Table 5. ANOVA analysis for hardness

Sources	DF	Seq SS	Adj SS	Adj MS	F-Value	P-Value	Remarks	R^2
Regression	2	234.135	234.135	78.045	11.77	0.011	Significant	0.890
Al6005	1	185.927	185.927	185.927	28.05	0.003	Significant	
Si_3N_4	1	135.413	135.413	185.927	23.05	0.003	Significant	
Graphite	1	45.927	45.927	45.927	6.93	0.046	Significant	
Die casting temp.	1	2.282	2.282	2.282	0.34	0.583	Insignificant	
Error	5	33.145	33.145	6.629				
Total	8	267.280						

Table 6. ANOVA analysis for thermal conductivity

Sources	DF	Seq SS	Adj SS	Adj MS	F-Value	P-Value	Remarks	R^2
Regression	3	38178	38178	212725.8	31.77	0.000	Significant	0.9226
Al6005	1	6763	7515	7515.2	18.76	0.003	Significant	
Die casting temperature	1	29467	10172	10172.1	25.40	0.001	Significant	
Power in watt	1	1947	1947	1947.3	4.86	0. 059	Insignificant	
Error	5	3204	3204	400.5				
Total	8	41383						

graphs that compare experimental and expected results for Al7475 with Si_3N_4/Gr composites for all combinations taken into consideration. The relationship between the values predicted by predictive models and the observed experimental outcomes is graphically represented by these graphs. With an error margin of less than 10%, the graphs and formulae highlight the little difference between the expected and actual values (Table 7 and 8). This tight alignment shows that the observed values and the projected spots nearly match. This study's were found to be robust and reliable, as seen by their low error rate, which also confirms their excellent predictive capabilities and acceptable accuracy. Additionally, the findings unequivocally show that adding grain refiners or modifiers greatly improves

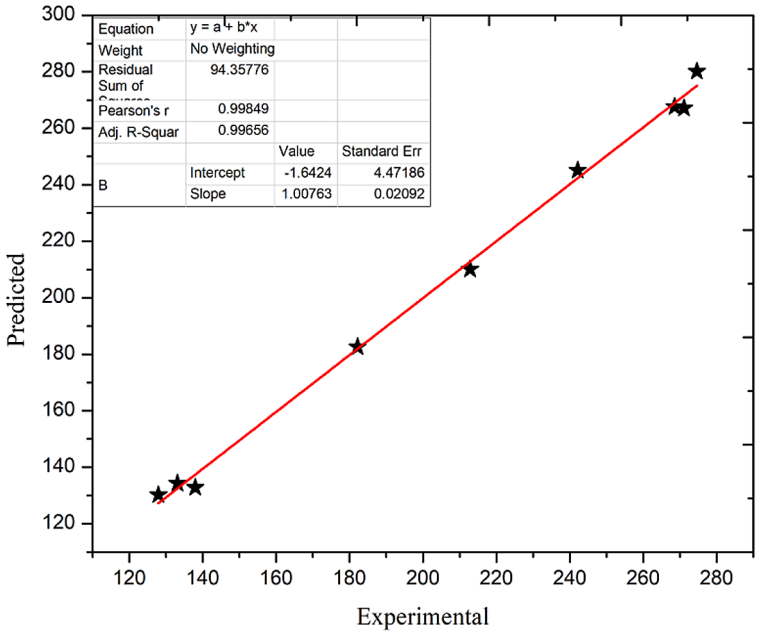

Figure 17. Predicted vs experimental analysis of thermal conductivity

Table 7. Measured vs predicted values of thermal conductivity

Sl. No.	Measured TC	Predicted TC	Error
1	274.63	290.132	-15.5024
2	271.08	236.113	34.9673
3	127.94	133.169	-5.2286
4	268.53	267.605	0.9248
5	212.84	205.094	7.7455
6	137.99	162.800	-24.8104
7	242.17	245.078	-2.9080
8	182.18	182.567	-0.3873
9	133.14	140.273	-7.1332

Table 8. Measured vs predicted values of hardness

Sl. No.	Measured hardness	Predicted hardness	Error
1	67.4	68.05	-0.65
2	68.7	69.36667	-0.66667
3	69.6	70.68333	-1.08333
4	69.3	70.03333	-0.73333
5	74.1	71.35	2.75
6	74.7	71.91667	2.783333
7	72.4	72.01667	0.383333
8	72.5	72.58333	-0.08333
9	71.2	73.9	-2.7

the materials' qualities. This result is noteworthy because it demonstrates how well these additives work to enhance the mechanical characteristics of the materials being studied.

CONCLUSIONS

The dispersion of graphite and Si_3N_4 in the Al7475 alloy enhanced its mechanical and thermal properties. Si_3N_4 improved the hardness and strength by inhibiting the movement of dislocations, while graphite contributed due to its solid lubrication behavior in yielding improved thermal conductivity. Among the tested combinations, the hybrid composite containing 5% Si_3N_4 and 5% Gr achieved the highest overall performance, achieving a hardness of 74.1 HV and thermal conductivity of 242.7 W/(m·°C). This composition delivered an optimum balance for strength, bonding quality, and uniform dispersion of the particles.

ANOVA results also validated the experimental findings by showing $R^2 > 98\%$ for hardness and $R^2 > 89\%$ for thermal conductivity, which indicates very good agreement among the experimental versus model-predicted values. The analysis confirmed that reinforcement content was the most statistically significant factor influencing both properties. The experimental and predicted results had an error margin of below 10%, ensuring the reliability and accuracy of the developed statistical models. Therefore, the study concludes that the Al7475–Si_3N_4/Gr hybrid composites can be successfully designed and optimized for future thermal management and lightweight aerospace applications.

REFERENCES

1. Ibrahim I. A., Mohamed F. A., Lavernia, E. J. *Particulate reinforced metal matrix composites – A review*. Journal of Materials Science, 1991; 26(5), 1137–1156. https://doi.org/10.1007/BF01176721
2. Raju L. S. and Kumar A., Influence of Al_2O_3 particles on the microstructure and mechanical properties of copper surface composites fabricated by friction stir processing, Defence Technology, Sep. 2014; 10(4), 375–383.
3. Moustafa E. B., Mikhaylovskaya A. V., Taha M. A., and Mosleh A. O., Improvement of the microstructure and mechanical properties by hybridizing the surface of AA7075 by hexagonal boron nitride with carbide particles using the FSP process, Journal of Materials Research and Technology, Feb. 2022; 17, 1986–1999.
4. Moustafa E. B., AbuShanab W. S., Ghandourah E., and Taha M. A., Microstructural, mechanical and thermal properties evaluation of AA6061/Al_2O_3-BN hybrid and mono nanocomposite surface, Journal of Materials Research and Technology, Nov. 2020; 9(6), 15486–15495.
5. Gugulothu B., Kumar P. S. S., Srinivas B., Ramakrishna A., and Vijayakumar S., Investigating the material removal rate parameters in ECM for Al5086 alloy-reinforced silicon carbide/flyash hybrid composites by using Minitab-18, Advances in Materials Science and Engineering, Nov. 2021; 2021, 2079811, 1–6.
6. Mazo M. A., Caballero A. C., and Rubio J., Silicon oxycarbide composites reinforced with silicon nitride and in situ formed silicon carbide, J. Eur. Ceram. Soc., Aug. 2024; 45(2025), 116828. https://doi.org/10.1016/j.jeurceramsoc.2024.116828
7. Sharath B. N., Madhu P., and Verma A., Enhancing tribological performance: A review of ceramic reinforced aluminium hybrid composites for high-temperature engineering applications, Hybrid Adv., Oct. 2023; 4, 100094, https://doi.org/10.1016/j.hybadv.2023.100094

8. Suvorova V. S. et al., Laser powder bed fusion of AlN and ZrN reinforced AlSi10Mg matrix composites: Effect of wettability and volume fraction on microstructure and mechanical properties, Int. J. Lightweight Mater. Manuf., Apr. 2025, Early Access. https://doi.org/10.1016/j.ijlmm.2025.04.002
9. Khalid M. Y., Umer R., and Khan K. A., Review of recent trends and developments in aluminium 7075 alloy and its metal matrix composites (MMCs) for aircraft applications, Results Eng., Aug. 2023; 20, 101372, https://doi.org/10.1016/j.rineng.2023.101372
10. Reddy K. S. K., Kannan M., and Karthikeyan R., Evaluation of mechanical and thermal properties of Aluminium -7475 reinforced with graphite and fly ash, in E3S Web Conf., 2021; 309, 01186, https://doi.org/10.1051/e3sconf/202130901186
11. Gangadharappa M., Geetha H. R., Manjunath N. K., Umesh G. L., and Shivakumar M. M., Study on n-TiB2 particulates reinforced Al7075 nano composite for soil nail applications: mechanical, wear, and fracture characterizations, Mater. Phys. Mech., 2024; 52(6), 101–113, https://doi.org/10.18149/MPM.5262024_9
12. Namdev N., Kukanur V., Bilgundi S., Bandi S. K., Vishwanath K. C., Kumar S. M., Valukula B., and Manjunatha T. H., Synthesis, hardness and tensile behavior of boron carbide reinforced Al6082 alloy composites for automotive applications, Braz. J. Dev., Jan. 2025; 11(1), 1–19, https://doi.org/10.34117/bjdv11n1-035
13. Gopalan K., Rajabathar S., Nagaral M., and Thippeswamy H. R., Evaluation of mechanical behaviour and tensile failure analysis of 8 wt.% of nano B4C particles reinforced Al2214 alloy nano composites, Manuf. Rev., 2022; 9, 31, https://doi.org/10.1051/mfreview/2022029
14. Jayaganthan R., Pramod R., and Nagaral M., Development of Aluminium 7075/Graphene nanoplatelets composites by stir casting for aerospace applications, Mater. Today, Proc., 2023; 80, 2405–2410, https://doi.org/10.1016/j.matpr.2023.07.178
15. Sukhdeve V. and Ganguly S. K. Utility of Taguchi based grey relational analysis to optimize any process or system 2015.
16. Montgomery, D.C. Design and Analysis of Experiments, 7th edition, John Wiley and Sons, Hoboken, NJ, USA. 2009.
17. Shankar V. K., Lakshmikanthan A., Selvan C. P., Girish B. M., Kunar B. M., Cuautle J. de J. A. F., Ramakrishna V. K., Malik V., Prediction of transient temperature at bit-rock interface using numerical modelling approach and optimization, International Journal on Interactive Design and Manufacturing (IJIDeM), https://doi.org/10.1007/s12008-023-01543-x
18. Varna K., Vijay Kumar S., Lakshmidevamma M. M., Benal M. M., Ercetin A., Murthy P., Comparison study of tensile strength characteristics of Al_2O_3 reinforced Al7075 and Al6061, 2022 Advances in Science and Engineering Technology, IEEE Xplore, 2022; 1–8.
19. Varna K., Vijay Kumar S., Lakshmidevamma M. M., Benal M. M., Prediction of Temperature during machinability of Al_2O_3 reinforced Al7075, Journal of Composite and Advanced Materials, International Information and Engineering Technology Associations, 2020; 30(5–6), 241–246.
20. Vijay Kumar S., Kunar B. M., Murthy Ch. S. N., Ramesh M. R. Measurement of bit-rock interface temperature and wear rate of the tungsten carbide drill bit during rotary drilling, Friction. 2020; 8(6), 1073–1082.
21. Sreenivasa Iyengar S. R., Sethuramu D., Ravikumar M., Mechanical, wear, and fracture behavior of Titanium Diboride (TiB_2) - Cerium Oxide (CeO_2) reinforced Al-6061 hot-rolled hybrid composites, Frattura ed Integrità Strutturale, 2023; 63, 289–300.
22. Ravikumar M., Suresh R., Study on mechanical and machinability characteristics of n-Al_2O_3/SiC-reinforced Al7075 composite by design of experiment technique, Multiscale and Multidisciplinary Modeling, Experiments and Design, 2023; 6, 747–760.
23. Sreenivasa Iyengar S. R., Sethuramu D., Ravikumar M., Study on micro-structure, hardness and optimization of wear characteristics of Al6061/TiB_2/CeO_2 hotrolled MMCs using Taguchi method, Frattura ed Integrità Strutturale, 2023; 65, 178–193.
24. Prakash T. B., Gangadharappa M., Somashekar S., Ravikumar M., Impact of nanoparticles (B4C-Al_2O_3) on mechanical, wear, fracture behavior and machining properties of formwork grade Al7075 composites, Frattura ed Integrità Strutturale, 2024; 69, 210–226.
25. Suchendra K. R., Sreenivasa Reddy M., Ravikumar M., Influence of quenching agents on mechanical, wear, and fracture characteristics of Al_2O_3 / MoS_2 Reinforced Al-6061 hybrid metal matrix composite (MMCs), Frattura ed Integrità Strutturale, 2023; 63, 122–133.
26. Ravikumar M., Naik R., Vinod B. R., Chethana K. Y., Rammohan Y. S., Study on nanosized Al_2O_3 and Al_2O_3-SiC on mechanical, wear and fracture surface of Al7075 composites for soil anchoring applications, Materials Physics and Mechanics. 2023; 51(6): 24–41.
27. RaviKumar M., VijayKumar S., Durga Prasad C., Sridevi G., Aprameya C. R., Kumar A., Bavan S., Adem A., Estimating and parametrically improving the microstructure, hardness, and wear resistance of SiC-CeO_2 reinforcements on hot rolled Al7075 hybrid composites, Results in Engineering 2025; 26, 104634.
28. Ravikumar M., Chethana K.Y., Vinod B.R., Suresh R., Nano sized SiC-Gr particulates reinforced Al7075 hybrid composite: Experimental studies and analysis of quenching agents, Jurnal Tribologi 2023; 38, 82–99.